Triazine-Based Liquid Crystal Dendrimers

Most triazine-based liquid crystalline (LC) dendrimers reported thus far are the main-chain LC macromolecules with long flexible chains at their periphery and attached to internal rigid or semi-rigid frameworks. Their formation of mesogenic phases often depends on the intermolecular face-to-face π–π interactions between dendritic molecules, which are unusual. Their mesogenic phases can also be formed by incorporation of mesogenic units to the dendritic skeletons through long flexible chains, as most side-chain LC dendrimers, in which the peripheral mesogenic units generally play the important roles. For main-chain triazine-based dendrimers, their morphology is maintained by restricted freedom of rigid or semi-rigid connecting units, and their formations of LC phases are therefore not straightforward to be controlled.

1. Introduction

Since the discovery of dendrimers in the late 1970s, [1] there has been substantial development in their synthesis and study of their physical properties. Dendrimers generally consist of a central core, linking bridges and peripheral groups. They can be efficiently prepared by iterative processes through convergent, divergent, and combined approaches as demonstrated in Scheme 1 [2]. Although dendrimers may have a branched architecture and three-dimensional spatial arrangement, their morphology is still predictable. Formed by controllable step-by-step and iterative processes, dendrimers are a class of macromolecules with several characteristics that polymers do not have, such as monodispersity, controllable sizes, and internal cavities [2]. In particular, various types of functionally designed groups can be attached at the periphery of dendrimers to give desired properties for this type of macromolecule. Therefore, dendrimers have been extensively investigated and are currently applied in various fields, including drug delivery [3][4][5][6][7][8][9], catalysis [10][11][12][13][14][15][16], light harvesting [17][18][19][20][21][22], and porous materials [23][24][25][26][27].
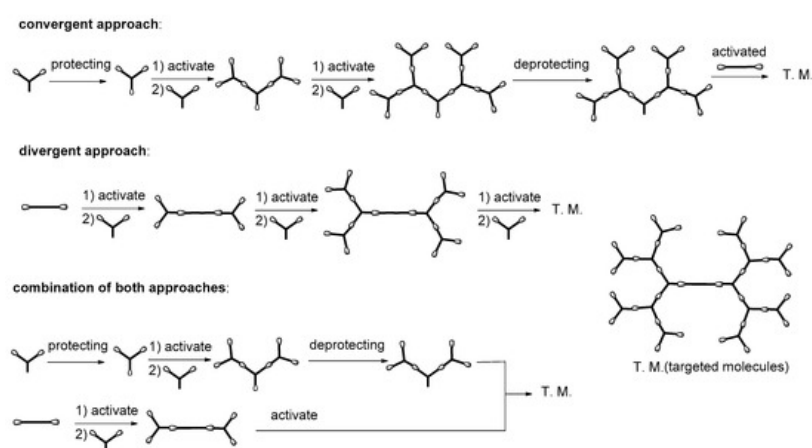
Scheme 1. Preparation of dendrimers by the convergent, divergent, and combined approaches.

With mesogenic units in the dendritic framework, dendrimers have also been observed to exhibit liquid crystal (LC) behaviors on thermal treatment. Compared with traditional LC usually with low molecular weight, LC dendrimers often have a higher molecular weight and exhibit columnar mesophases on thermal treatment and are 2-D regular materials, thus yielding better self-assembling ability in a long-range domain and which have usefulness as solvating candidates in opto-electronic devices [28][29][30][31][32][33][34]. LC dendrimers can generally be divided into side-chain dendrimers in which the mesogenic units are incorporated at the periphery of molecules and main-chain dendrimers in which the mesogenic moieties are designed as linking moieties within the internal framework. Most LC dendrimers are side-chain LCs with flexible cores or linking units and peripheral mesogenic units linked to the internal dendritic structures through long flexible chains. The mesogenic units are important in inducing their LC behavior, and this type of LC dendrimer mostly consists of PMAMA (polyamidoamine), PPI (polypropylimine), Si-derivatives (siloxanes, carbosilanes, and carbosilazanes), and

polyester as their dendritic network, all of which have been reviewed extensively [2][35][36][37][38]. Special functional moieties, such as fullerene and ferrocene, may be incorporated in side-chain LC dendrimers for particular properties as reported in literatures [2][36][39]. There are fewer main-chain LC dendrimers [40][41][42][43][44][45] than side-chain LC dendrimers because mesogenic moieties are used as bridging units in their internal structures, leading to a rigid or semi-rigid dendritic framework in the main-chain LC dendrimers in which flexible alkyl chains are frequently grafted at the periphery to increase their solubility in organic solvents. Therefore, in contrast to side-chain LC dendrimers in which the LC phases are mostly induced by the peripheral mesogenic units, both the rigid or semi-rigid internal frameworks and flexible peripheral chains are all important in inducing mesophases for the main-chain LC dendrimers [2][36][37], and this leads the formation of mesophases of the main-chain LC dendrimers to be difficult to control. As in the rod-like liquid crystals, the ionic, H-bond, and metallo interactions are also extensively employed in LC dendrimers, which also consist of side-chain and main-chain types of LC materials, depending on whether their mesogenic units are incorporated in the internal framework or at the periphery of dendritic network, which have been reviewed in the literature [46][47][48].

Cyanuric chloride, a simple heterocycle with three reactive sites on its ring, can be used as a branching unit for efficiently preparing dendrimers. For instance, the first chloro substituent can be replaced by alkylamines at 0 °C, and subsequently, the second and the third substituents can undergo similar substitutions at room temperature and above 60 °C, respectively (Scheme 2) [49][50]. The triazine-based dendrimers were first prepared by Takagi [51] and later investigated by others [52][53]. Little progress on LC dendrimers based on the triazine unit has been reported since then. To the best of our knowledge, in 2008, Lai and co-workers were the first to report LC dendrimers on the basis of the 1,3,5-triamino-s-triazine unit [54]. Kotha and colleagues also prepared 1,3,5-triphenyl-s-triazine-based dendrimers, which exhibited a columnar phase after being mixed with 1:1 molar ratio of trinitrofluorenone [55]. However, there has been less study of triazine-based LC dendrimers, and most are main-chain types of LC dendrimers. Induction of the LC phases of triazine-based dendrimers can be achieved by manipulating the molecular morphology of the dendrimer themselves or by adding extra components to form an LC dendritic mixture by intermolecular H-bond or face-to-face π–π interactions. By reviewing this system, we hope to guide future work in this field.

Scheme 2. Reaction of amines with cyanuric chlorides at different temperatures.

2. Formation of Triazine-Based LC Dendrimers by Manipulating Their Molecular Morphology

2.1. LC Dendrimers with C_2 Symmetry

The LC dendrimer with a C_2-symmetry on the basis of a 1,3,5-triamino-s-triazine unit was first reported by Lai and colleagues [54]. They prepared the fourth generation LC dendrimer **1** by the convergent approach (**Figure 1**), with a single molecular weight of ~12,479. Compound **1** is a monotropic material, showing no mesophase during heating but a columnar hexagonal phase between ~160 and ~143 °C on cooling. Additionally, compound **1** did not show any significant absorbance beyond 280 nm in the UV-vis spectrum and started to decompose at 300 °C under nitrogen by TGA analysis, which is an important characteristic required for opto- and electro-applications. However, the third generation triazine-based dendrimer **2** did not exhibit mesogenic behavior on thermal treatment, isotropic at ~133 °C on heating, and crystallized at ~98 °C on cooling. Computer simulations for the conformations of dendrimers **1** and **2** showed that the steric effect from the peripheral skeleton of **1** is more significant than that of **2** [54], i.e., the dendritic conformation of **1** is less coplanar due to congestion between the branched mainframe, thus reducing the face-to-face π–π interactions between dendritic molecules and forming the columnar phase on thermal treatment. Compared with traditional disk molecules, dendrimer **1** with a C_2-symmetry having a columnar LC phase on cooling, is unusual. To exhibit columnar mesophases, the traditional C_2-symmetry molecules may consist of a macrocyclic core [56][57]. Introducing a chiral core to result in helical stacking columns by modulating the intermolecular π–π interaction between molecules is another approach [58].
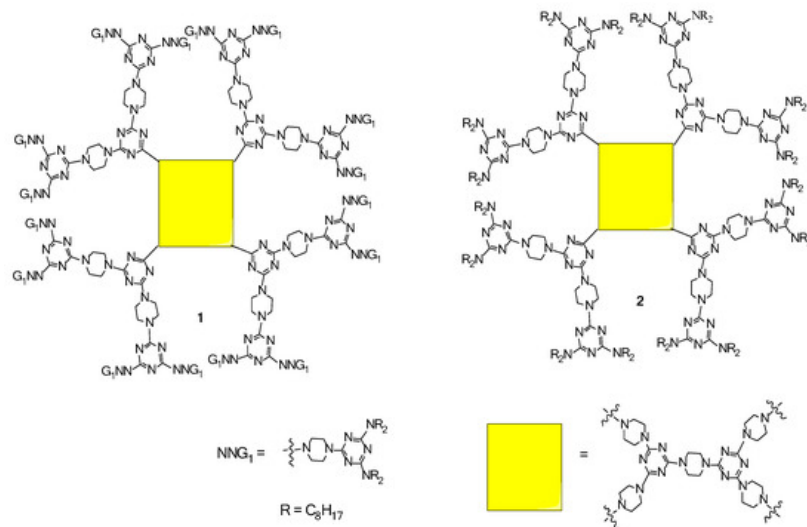
Figure 1. Structures of dendrimers (**1**) and (**2**) with C_2-symmetry.

2.2. LC Dendrimers with C₃ Symmetry

In addition, deforming the planarity of trigonal disk molecules to reduce face-to-face π–π interactions in traditional molecules can also lead to the formation of columnar mesophases [59]. Therefore, changing the shape of the rigid cores can be an efficient approach for preparing dendrimers with columnar LC phases, and thus two C_3-symmetry dendrimers based on a triazine unit have been reported (**Figure 2**) [60]. Dendrimer **3**, with a molecular weight of ~9248, is a monotropic material, which did not exhibit any mesogenic behavior on heating but showed a columnar phase between ~137 and ~100 °C on cooling. Dendrimer **4** exhibited a columnar phase from ~141 to ~173 °C on heating and from ~168 to ~136 °C on cooling.
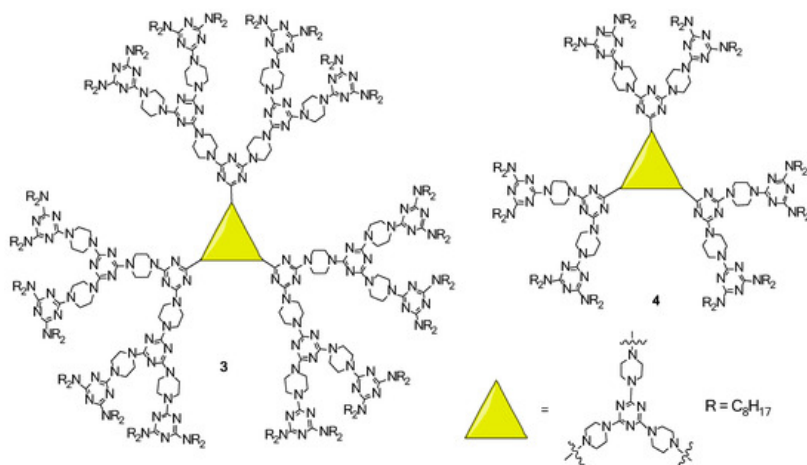

Figure 2. Structures of dendrimers (**3**) and (**4**) with C_3-symmetry.

As demonstrated by dendrimers **1** and **2**, high molecular weight deforms the planar mainframe of dendritic molecules and leads to the formation of LC phases on thermal treatment. However, the molecular weight of dendrimer **4** (~4423) is much smaller than that of dendrimer **2** (~6034). Apparently, the C_2-to-C_3 approach significantly changes planarity of the internal mainframe of dendrimers. Thus **4** exhibits a columnar LC phase during the thermal process although there is less congestion from the dendritic mainframe when compared with that of **2**.

2.3. LC Dendrimers with the Loss of C_2 Symmetry by Changing the Peripheral Groups

Reducing the intermolecular face-to-face π–π interactions between the molecules of triazine-based dendrimer seems to be a good strategy for forming mesogenic phases on thermal treatment. According to literature [61], mixing two pure components can reduce the molecular interaction in the solid state, and thus lowers the melting point of the mixture. For example, the m.p. of (R)-(−)-2-amino-1-propanol is ~24–26 °C, which is the same as that of (S)-(+)-2-amino-1-propanol, but the m.p. of the 1:1 mixture of these two components drops to ~8–10 °C. Accordingly, four triazine-based LC dendrimers were prepared (**Figure 3**) [62]. Dendrimer **5**, with the loss of the C_2-symmetry, exhibited a columnar phase from ~95 to ~152 °C on heating and from ~147 to ~64 °C on cooling. Dendrimer **6**, also with the loss of the C_2-symmetry, is a monotropic material, only showing a columnar phase between ~123 and ~145 °C on heating. Dendrimers **7** and **8**, with a C_2-symmetry, did not exhibit any mesogenic phase on thermal treatment. Dendrimer **7** became isotropic at ~132 °C

on heating and crystallized at ~117 °C on cooling; and dendrimer **8** became isotropic at ~229 °C on heating and solidified at ~221 °C on cooling. Dendrimers **5**, **6**, **7**, and **8** all have similar molecular weights of ~2368, ~2030, ~2813, and ~2363, respectively. Based on the molecular simulation investigations [62], they are almost co-planar and the congestions between their dendritic frameworks are negligible. However, dendrimers **5** and **6** are isomeric. As shown in **Figure 4**, dendrimers **5** or **6**, in principle, can be produced from the combination of the corresponding Cl-dendron and piperazino-dendron, respectively. Each dendron consists of at least four isomers, and therefore, dendrimers **5** and **6** have many isomers in their solid stackings, reducing their intermolecular face-to-face π–π interactions and forming LC phase during the thermal process.
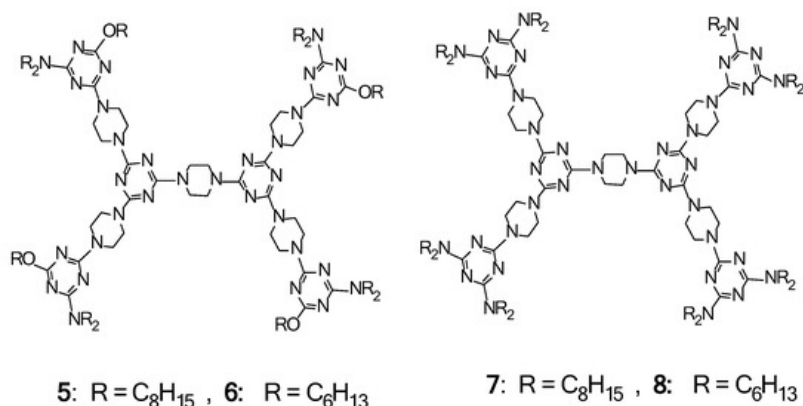

5: R = C_8H_{15} , **6**: R = C_6H_{13} **7**: R = C_8H_{15} , **8**: R = C_6H_{13}

Figure 3. Structures of dendrimers (**5**) and (**6**) without a C_2-symmetry and structures of dendrimers (**7**) and (**8**) with a C_2-symmetry.
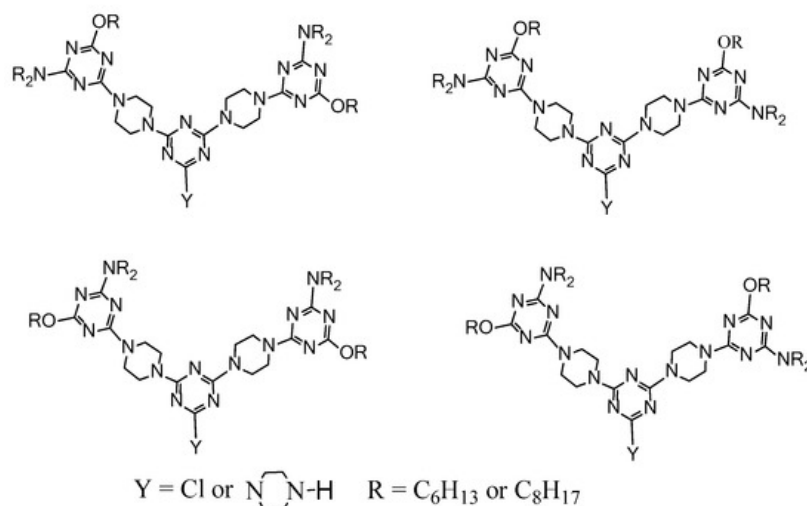

Y = Cl or N◯N-H   R = C_6H_{13} or C_8H_{17}

Figure 4. Structural isomers of dendrons to form dendrimers (**5**) and (**6**).

2.4. LC Dendrimers with the Loss of C_2 Symmetry by Changing the Central Cores

Partially changing the peripheral group to break C_2-symmetry of molecules can lead dendrimers to contain isomers, and face-to-face π–π interactions between dendritic molecules are thus modulated to form the LC phase with thermal treatment. This strategy can also be applied to central linkers of dendrimers. With the peripheral group fixed by the dialkylamino units, the central linker is modulated as C_5H_{10}, C_4H_8, C_3H_6, and C_2H_4 (**Figure 5**) [63]. Dendrimers **9** and **11**, with the odd-number carbon linker in the dendritic core, are LCs. Dendrimer **9** was observed to exhibit a columnar phase from ~109 to ~168 °C on heating and from ~146 to ~87 °C on cooling. Dendrimer **11** showed a columnar phase between ~107 and ~144 °C on heating and between ~115 and ~81 °C on cooling. Dendrimers **10** and **12** with the even-number carbon linker in the dendritic core are not liquid crystalline. The solid-phase-to-isotropic-phase (solid-to-iso) transition temperatures for dendrimers **10** and **12** are ~132 and ~147 °C, respectively, on heating, and the isotropic-phase-to-solid-phase (iso-to-solid) transition temperatures for **10** and **12** are ~100 and ~90 °C, respectively, on cooling.

$R = C_8H_{17}$
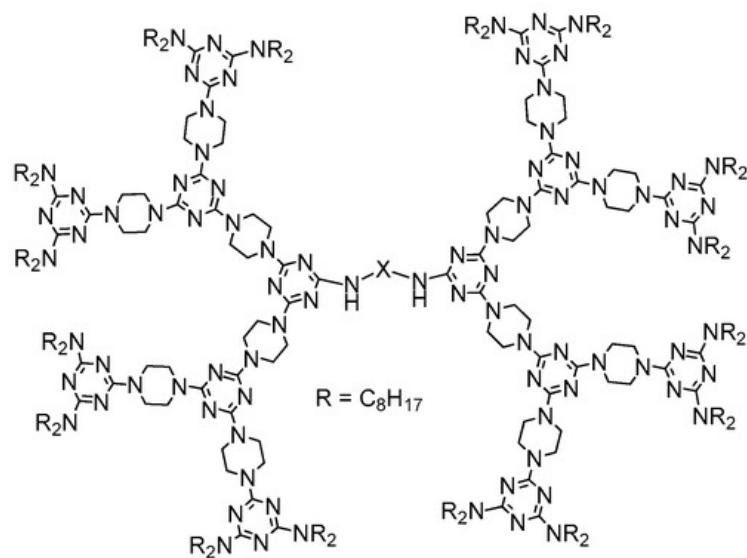
9: X= C_5H_{10}, **10**: X= C_4H_8, **11**: X= C_3H_6, **12**: X= C_2H_4

Figure 5. Structures of dendrimers (**9**–**12**).

Molecular weights for dendrimers **9**–**12** are similar: ~6050, ~6036, ~6022, and ~6008, respectively. A computer simulation for molecular conformations of dendrimers **9** and **10** showed that **9** is asymmetrical and **10** is symmetrical along with the central linkers, and a diagram can show their differences [63]. As shown in **Figure 6**, dendrimer **10**, with a 4-carbon linker in the dendritic core, allows the dendronic halves to be located at the *anti*-position of the C_4H_8 linker to reduce repulsions between Hs (at C_2 and C_3) and the dendronic halves. Therefore, the molecular conformation of **10** is almost symmetrical. Accordingly, dendrimer **11** with a 3-carbon linker leads both the dendronic halves to exist in the *syn*-position of the C_3H_6 linker to reduce corresponding repulsions; in this conformation, two isomers of dendrimer **11** should exist since the left dendronic half may be on the top or bottom of the right dendronic half (**Figure 6**). Because of the isomeric effect, the intermolecular face-to-face π–π interactions are reduced in the solid stacking, and the columnar phases of dendrimers **9** and **11** are thus formed on thermal treatment. To further understand the isomeric effect on influencing their stackings in LC state, their molecular volumes (V_m) and cell volumes (V_{cell}) were calculated on the basis of powder-XRD data of dendrimers **9** and **11** [63]. Since the calculated volumes are temperature-dependent, and the XRD data for **9** and **11** were collected at different temperatures, the V_m/V_{cell} ratios, instead of V_m or V_{cell}, were compared to remove the temperature factor. The V_m/V_{cell} ratios of **9** and **11** were calculated to be ~1.03 and ~0.95, respectively. For the non-mesogenic compounds **10** and **12**, crystalline XRD data were also used for calculation, assuming that both formed the columnar hexagonal crystalline phase; the V_m/V_{cell} ratios of **10** and **12** were estimated to be ~0.92 and ~0.87, respectively.
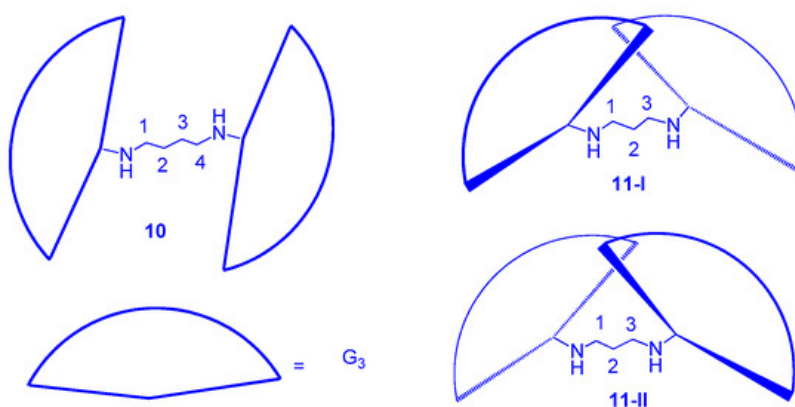

Figure 6. Isomers of dendrimers (**10**) and (**11**).

The ratios of V_m/V_{cell} for **9** and **11** are larger than those for **10** and **12**, indicating that the stackings of **9** and **11** in the solid state are somewhat looser than those of **10** and **12**. This further indicates that the isomeric effect on dendrimers can probably modulate the face-to-face π–π interactions between dendritic molecules.

As indicated previously, the repulsion between dendronic halves and the Hs (at C_2 or C_3) significantly influences the conformation of dendrimer **10**. If the central linker of **10** was methylated on nitrogen, then the repulsion between Me and

the Hs (at C_2 or C_3) should increase, although the repulsion should be smaller than that between the dendronic halves and the corresponding Hs (at C_2 or C_3). However, this should convert several of the dendronic halves at the *anti*-position of C_4H_8 linker to the *syn*-position. Specifically, dendrimer **13** should have three isomers in the solid state, as shown in **Figure 7** [64], although most of the **13** exists as the form of isomer **13-I** and, as expected, dendrimer **13** exhibited a columnar phase on thermal treatment (**Figure 8**). The mesogenic range is from ~111 to ~123 °C on heating and from ~115 to ~94 °C on cooling. Accordingly, dendrimer **14** has three isomers in the solid state but showed only a columnar phase between ~94 and ~72 °C on cooling without showing any mesogenic behavior on heating.
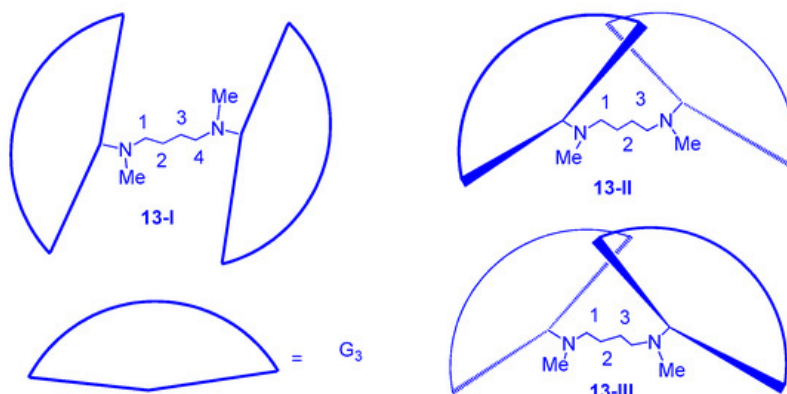

Figure 7. Isomers of dendrimers (**13-I**), (**13-II**), and (**13-III**).
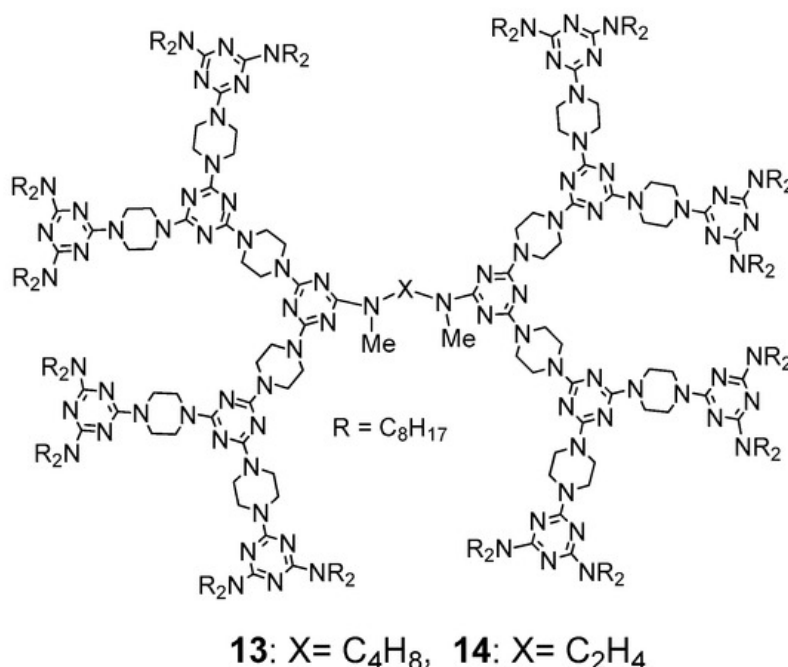

Figure 8. Structures of dendrimers (**13**) and (**14**).

The solid-to-iso transition temperatures of dendrimers **10** and **12** on heating are ~132 and ~147 °C, respectively, which are higher than those of corresponding dendrimers **13** and **14** (~118 and 123 °C, respectively). This indicates that methylation of nitrogen in the central linker affects their molecular morphology and somewhat loosens their solid stacking. Based on the powder-XRD data of dendrimers **13** and **14**, their ratios of V_m/V_{cell} were also calculated. The V_m/V_{cell} ratio of **13** was ~0.92, similar to that of **10** (~0.92) and the V_m/V_{cell} ratio of **14** was ~0.80, which is smaller to that of **12** (~0.87).

Although methylation of nitrogens in the central linker of dendrimers converts non-mesogenic **10** and **12** to become mesogenic **13** and **14**, respectively, the isomeric effect seems to not be significant in reducing intermolecular face-to-face π–π interactions, allowing dendrimers **13** and **14** to be looser in the solid stacking than dendrimers **10** and **12**. Based on the optimal conformation of **13** [64], it was discovered that four intramolecular H-bond interactions arise between N_a (a = 7, 8, 9, 10) and H (at C_b; b = 1, 4, 5, 6), respectively, as shown in **Figure 9**. Accordingly, only two intramolecular H-bond interactions arise between N_a (a = 5, 6) and H (at C_b; b = 1, 4,) in dendrimer **10**. Therefore, dendrimer **13** that mostly exists in the form of **13-I** should be more rigid and is less distorted than dendrimer **10**, and therefore the void space inside the solid stacking of **10** should be larger than that inside the dendritic framework of **13-I**. However, because of the isomeric effect, the face-to-face π–π interactions between dendritic molecules of **13** is reduced and therefore its dendritic framework is fluffier. As a result, dendrimers **10** and **13** have almost the same V_m/V_{cell} ratio (~0.92) on the basis of

balancing the two conflicting factors. When the central linker is shortened, congestion from dendritic halves of **12** is more vigorous and the distortion allows dendrimer **12** to become more porous. Therefore, the V_m/V_{cell} ratio of **12** (~0.87) is larger than that of **14** (~0.80).
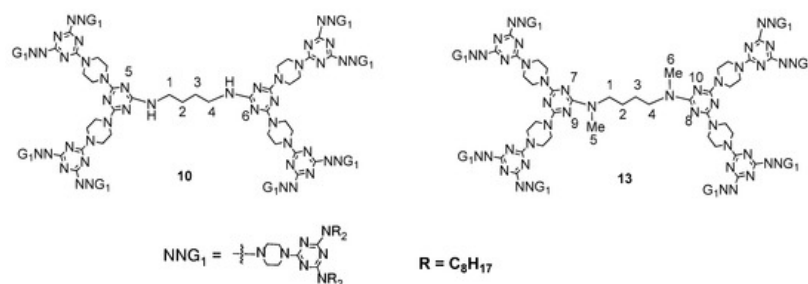

Figure 9. The numbering on carbons for indicating intramolecular H-bond interactions between H and N of dendrimers (**10**) and (**13**).

The central linkers in triazine-based dendrimers significantly influence their morphology and consequently affect the formation of the mesophase during the thermal process. Instead of N-alkylation of an even-number carbon central linker, this strategy was also undertaken to an odd-number carbon central linker. As dendrimer **11** has already been observed to exhibit a columnar phase on thermal treatment, a strong CN polar group was incorporated in the central linker to investigate its influence on the mesogenic behavior. Dendrimers **15** and **16** were therefore further prepared for studying their LC properties (**Figure 10**) [65]. Dendrimer **15** exhibited a columnar phase between ~102 and ~118 °C on heating and between ~115 and ~82 °C on cooling. Dendrimer **16** showed a columnar phase from ~88 to ~144 °C on heating and from ~138 to ~68 °C on cooling. Compared with the DSC behaviors of **11**, the solid-to-iso transition temperature of **15** (~118 °C) was lower than that of **11** (~144 °C) on heating, indicating that the alkylation on N in the central linker increased the steric congestion of triazine-based dendrimer and somewhat loosened their solid stacking as shown in the study of dendrimers **10**, **12**, **13** and **14**. The solid-to-iso transition temperature of **16** (~144 °C) was similar to that of **11** (~144 °C), and the mesogenic range of **16** on cooling (from ~138 to ~68 °C) was broader than that of **11** (from ~115 to ~81 °C). The CN group in the central linker not only lowered the solidifying temperature but also raised the isotropic-phase-to-columnar-mesophase (iso-to-col) transition temperature on cooling. In principle, the steric congestion from benzyl moiety in the central linker of dendrimers **15** should not differ from and 4-cyanobenzyl moiety in **16**, but their mesogenic behaviors on thermal treatment are significantly different. The strong polarity of the CN group strengthens intermolecular interactions between face-to-face dendritic molecules. For further understanding, the V_m/V_{cell} ratios of **15** and **16** were estimated on the basis of their powder-XRD data as ~0.80 and ~0.98, respectively. The V_m/V_{cell} ratio of dendrimer **16** was larger than that of **11** (~0.95), but that of dendrimer **15** was smaller, indicating that the loose order of their stacking is **16** > **11** > **15**. As dendrimers **11**, **15**, and **16** all show a columnar phase in the mesogenic range, the face-to-face distances between two dendritic molecules (d_{slice}) for **11**, **15**, and **16** can be obtained from the powder-XRD data in a similar manner and are calculated to be 13.14, 13.28, and 13.68 Å, respectively. The V_m/V_{cell} ratios and d_{slice} distances show that the strong polarity of CN group significantly increased the face-to-face distance between dendritic molecules within columns. This reasonably explains that the col-to-solid transition temperature on cooling of **16** is lower than those of **11** and **15**. However, as indicated previously, the solid-to-iso transition temperature of **16** (~144 °C) is similar to that of **11** (~144 °C) on heating, which can also be ascribed to the strong polarity of the CN group. During the heating process, the strong intermolecular polar-to-polar interactions within columns led dendrimer **16** to have the same solid-to-iso transition temperature as **11**, although the stacking of **16** was looser. Neither dendrimer **11** nor **15** contains any functional group in the central linker, but the d_{slice} distance of **15** within columns is 13.28 Å, only slightly larger than that of **11** (13.14 Å). The more void space between dendritic molecules of **15** is occupied by the benzyl group, which results in the lower V_m/V_{cell} ratio of **15** (0.80) versus that of **11** (0.95). Since the d_{slice} distances of **11** and **15** do not differ from each other, the mesophase ranges of both dendrimer are also similar to each other.
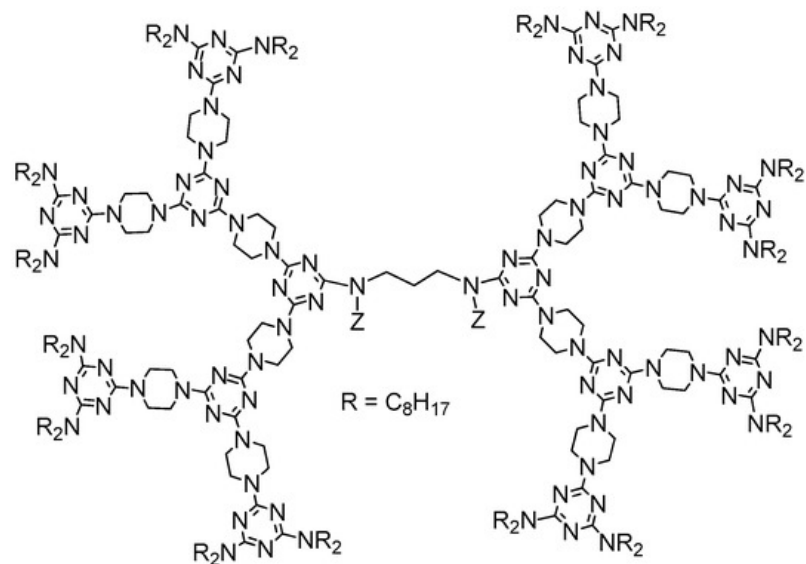
15: Z= CH$_2$-C$_6$H$_5$, 16: Z= CH$_2$-C$_6$H$_4$CN

Figure 10. Structures of dendrimers (**15**) and (**16**).

3. Formation of Triazine-Based LC Dendrimers by Adding Extra Components

3.1. Formation of LC Dendrimers by Intermolecular π–π Interaction

In addition to manipulating the morphology of dendritic molecules to form their LC phase, mixing extra components to non-liquid-crystalline (non-LC) triazine-based dendrimers can lead to the mesophase formation. Dendrimers **17** and **18** were reported to be non-LC on thermal treatment (**Figure 11**) [55]. Compound **17** became isotropic at ~66 °C on heating but no transition was observed on cooling. Compound **18** became isotropic at ~57 °C on heating and crystallized at ~32 °C on cooling. After mixing with 1:1 molar ratio of trinitrofluorenone (**TNF**), the mixture of **17**-**TNF** showed a columnar phase between ~56 and ~78 °C on heating but still no transition was observed on cooling. The mixture of **18**-**TNF** exhibited a columnar phase from ~51 to ~102 °C on heating and from ~97 °C to room temperature on cooling [55]. It is believed that **TNF** forms a complex mixture with **17** or **18** through the face-to-face π-π interactions, thereby adjusting the distance between dendritic molecules and showing LC phases on thermal treatment.
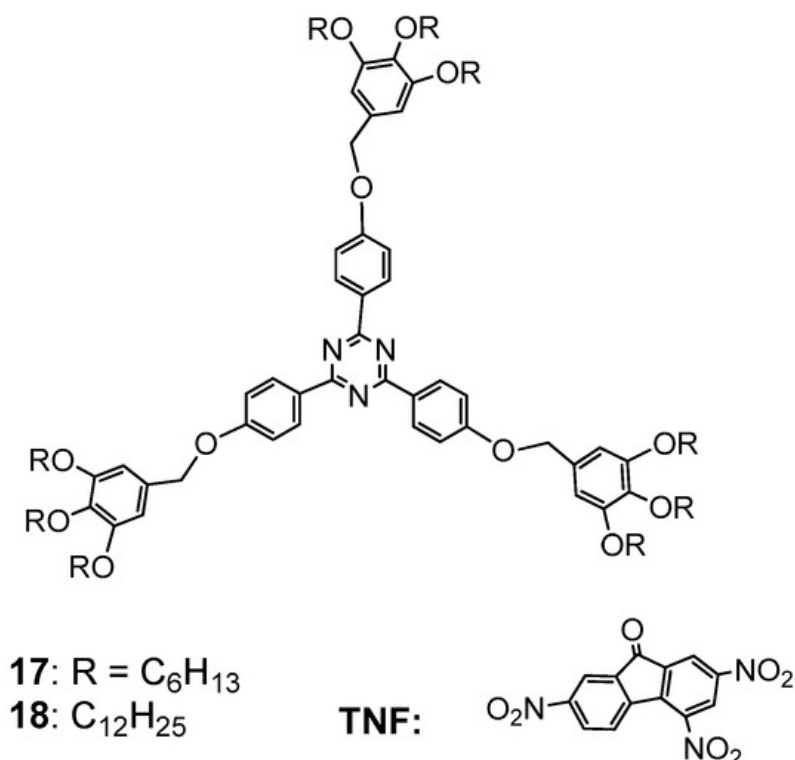

17: R = C$_6$H$_{13}$
18: C$_{12}$H$_{25}$ TNF:

Figure 11. Structures of dendrimers (**17**) and (**18**).

3.2. Formation of LC Dendrimers by Intermolecular H-Bond Interaction

Apart from the face-to-face π–π interactions, the LC dendritic mixtures can also be formed by the intermolecular H-bond interaction. Mixing 2,4-diamino-6-dodecyl-1,3,4- triazine with carboxylic acid-containing dendron in a 1:3 ratio generates H-bonded dendrimers **19** and **20**, as shown in **Figure 12** [66]. The acid-containing dendrons **21** and **22** did not exhibit any mesophase on thermal treatment. Compound **21** showed only a glass-phase-to-isotropic-phase (glass-to-iso) transition temperature at ~52 °C on heating, and compound **22** showed a glass-to-iso transition temperature at ~46 °C on heating. Instead of a columnar phase, dendrimer **19** exhibited a nematic phase between ~4 and ~35 °C on heating, and dendrimer **20** was observed to exhibit a SmA phase from ~43 and ~70 °C on heating. Neither dendrimers nor dendrons were reported to show any mesophase on cooling. A carbazole unit was incorporated in dendrimers and dendrons for studying their photoconductivities, but the performances of dendrons **21** and **22** were slightly better than those of dendrimers **19** and **20**, respectively.
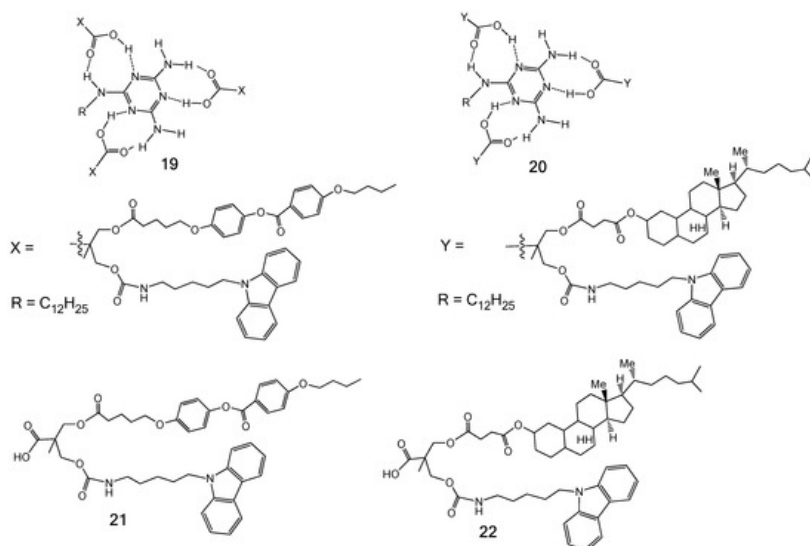

Figure 12. Structures of dendrimers (**19**) and (**20**) and and dendrons (**21**) and (**22**).

References

1. Tomalia, D.A.; Fréchet, J.M.J. Discovery of dendrimers and dendritic polymers: A brief historical perspective. J. Polym. Sci. A Polym. Chem. 2002, 40, 2719–2728.

2. Caminade, A.-M.; Turrin, C.-O.; Laurent, R.; Ouali, A.; Delavaux-Nicot, B. Dendrimers: Towards Catalytic, Material and Biomedical Uses; Wiley: New York, NY, USA, 2011.

3. Janaszewska, A.; Lazniewska, J.; Trzepiński, P.; Marcinkowska, M.; Klajnert-Maculewicz, B. Cytotoxicity of Dendrimers. Biomolecules 2019, 9, 330.

4. Chauhan, A.S. Dendrimers for Drug Delivery. Molecules 2018, 23, 938.

5. Sherje, A.P.; Jadhav, M.; Dravyakar, B.R.; Kadam, D. Dendrimers: A versatile nanocarrier for drug delivery and targeting. Int. J. Pharm. 2018, 548, 707–720.

6. Kaur, D.; Jain, K.; Mehra, N.K.; Kesharwani, P.; Jain, N.K. A review on comparative study of PPI and PAMAM dendrimers. J. Nanopart. Res. 2016, 18, 146.

7. Kesharwani, P.; Jain, K.; Jain, N.K. Dendrimer as nanocarrier for drug delivery. Prog. Polym. Sci. 2014, 39, 268–307.

8. Madaan, K.; Kumar, S.; Poonia, N.; Lather, V.; Pandita, D. Dendrimers in drug delivery and targeting: Drug-dendrimer interactions and toxicity issues. J. Pharm. Bioallied Sci. 2014, 6, 139–150.

9. Mignani, S.; El Kazzouli, S.; Bousmina, M.; Majoral, J.-P. Expand classical drug administration ways by emerging routes using dendrimer drug delivery systems: A concise overview. Adv. Drug Deliv. Rev. 2013, 65, 1316–1330.

10. Liu, Y.; Lopes, R.P.; Lüdtke, T.; Di Silvio, D.; Moya, S.; Hamon, J.-R.; Astruc, D. "Click" dendrimer-Pd nanoparticle assemblies as enzyme mimics: Catalytic o-phenylenediamine oxidation and application in colorimetric H2O2 detection. Inorg. Chem. Front. 2021, 8, 3301–3307.

11. Yamamoto, K.; Imaoka, T.; Tanabe, M.; Kambe, T. New Horizon of Nanoparticle and Cluster Catalysis with Dendrimers. Chem. Rev. 2020, 120, 1397–1437.

12. Tang, Y.-H.; Cangiotti, M.; Kao, C.-L.; Ottaviani, M.F. EPR Characterization of Copper(II) Complexes of PAMAM-Py Dendrimers for Biocatalysis in the Absence and Presence of Reducing Agents and a Spin Trap. J. Phys. Chem. B 2017, 121, 10498–10507.

13. Neumann, P.; Dib, H.; Caminade, A.-M.; Hey-Hawkins, E. Redox Control of a Dendritic Ferrocenyl-Based Homogeneous Catalyst. Angew. Chem. Int. Ed. 2015, 54, 311–314.

14. Twyman, L.J.; King, A.S.H.; Martin, I.K. Catalysis inside dendrimers. Chem. Soc. Rev. 2002, 31, 69–82.

15. Astruc, D.; Chardac, F. Dendritic Catalysts and Dendrimers in Catalysis. Chem. Rev. 2001, 101, 2991–3024.

16. Crooks, R.M.; Zhao, M.; Sun, L.; Chechik, V.; Yeung, L.K. Dendrimer-Encapsulated Metal Nanoparticles: Synthesis, Characterization, and Applications to Catalysis. Acc. Chem. Res. 2001, 34, 181–190.

17. Concellón, A.; Termine, R.; Golemme, A.; Romero, P.; Marcos, M.; Serrano, J.L. High hole mobility and light-harvesting in discotic nematic dendrimers prepared via 'click' chemistry. J. Mater. Chem. C 2019, 7, 2911–2918.

18. Yim, D.; Sung, J.; Kim, S.; Oh, J.; Yoon, H.; Sung, Y.M.; Kim, D.; Jang, W.-D. Guest-Induced Modulation of the Energy Transfer Process in Porphyrin-Based Artificial Light Harvesting Dendrimers. J. Am. Chem. Soc. 2017, 139, 993–1002.

19. Nantalaksakul, A.; Reddy, D.R.; Bardeen, C.J.; Thayumanavan, S. Light Harvesting Dendrimers. Photosyn. Res. 2006, 87, 133–150.

20. Balzani, V.; Ceroni, P.; Maestri, M.; Vicinelli, V. Light-harvesting dendrimers. Curr. Opin. Chem. Biol. 2003, 7, 657–665.

21. Adronov, A.; Fréchet, J.M.J. Light-harvesting dendrimers. Chem. Comm. 2000, 18, 1701–1710.

22. Gilat, S.L.; Adronov, A.; Fréchet, J.M.J. Light Harvesting and Energy Transfer in Novel Convergently Constructed Dendrimers. Angew. Chem. Int. Ed. 1999, 38, 1422–1427.

23. Wang, Y.; He, X.; Lu, Q. Polyamidoamine dendrimer functionalized cellulose nanocrystals for CO2 capture. Cellulose 2021, 28, 4241–4251.

24. El Kadib, A.; Katir, N.; Bousmina, M.; Majoral, J.P. Dendrimer–Silica hybrid mesoporous materials. New J. Chem. 2012, 36, 241–255.

25. Bonaccorsi, L.; Lombardo, D.; Longo, A.; Proverbio, E.; Triolo, A. Dendrimer Template Directed Self-Assembly during Zeolite Formation. Macromolecules 2009, 42, 1239–1243.

26. Yoo, S.; Lunn, J.D.; Gonzalez, S.; Ristich, J.A.; Simanek, E.E.; Shantz, D.F. Engineering Nanospaces: OMS/Dendrimer Hybrids Possessing Controllable Chemistry and Porosity. Chem. Mater. 2006, 18, 2935–2942.

27. Kriesel, J.W.; Tilley, T.D. Dendrimers as Building Blocks for Nanostructured Materials: Micro- and Mesoporosity in Dendrimer-Based Xerogels. Chem. Mater. 1999, 11, 1190–1193.

28. Martínez, N.P.; Inostroza-Rivera, R.; Durán, B.; Molero, L.; Bonardd, S.; Ramírez, O.; Isaacs, M.; Díaz Díaz, D.; Leiva, A.; Saldías, C. Exploring the Effect of the Irradiation Time on Photosensitized Dendrimer-Based Nanoaggregates for Potential Applications in Light-Driven Water Photoreduction. Nanomaterials 2019, 9, 1316.

29. Avila-Salas, F.; Pereira, A.; Rojas, M.A.; Saavedra-Torres, M.; Montecinos, R.; Bonardd, S.; Quezada, C.; Saldías, S.; Díaz Díaz, D.; Leiva, A.; et al. An experimental and theoretical comparative study of the entrapment and release of dexamethasone from micellar and vesicular aggregates of PAMAM-PCL dendrimers. Eur. Polym. J. 2017, 93, 507–520.

30. Axenov, K.V.; Laschat, S. Thermotropic Ionic Liquid Crystals. Materials 2011, 4, 206–259.

31. Rosen, B.M.; Wilson, C.J.; Wilson, D.A.; Peterca, M.; Imam, M.R.; Percec, V. Dendron-Mediated Self-Assembly, Disassembly, and Self-Organization of Complex Systems. Chem. Rev. 2009, 109, 6275–6540.

32. Goodby, J.W.; Saez, I.M.; Cowling, S.J.; Görtz, V.; Draper, M.; Hall, A.W.; Sia, S.; Cosquer, G.; Lee, S.-E.; Raynes, E.P. Transmission and Amplification of Information and Properties in Nanostructured Liquid Crystals. Angew. Chem. Int. Ed. 2008, 47, 2754–2787.

33. Kim, H.-J.; Jung, E.-Y.; Jin, L.Y.; Lee, M. Solution Behavior of Dendrimer-Coated Rodlike Coordination Polymers. Macromolecules 2008, 41, 6066–6072.

34. Inoue, K. Functional dendrimers, hyperbranched and star polymers. Prog. Polym. Sci. 2000, 25, 453–571.

35. Hernández-Ainsa, S.; Barberá, J. Fluorinated liquid crystalline dendrimers. J. Fluor. Chem 2015, 177, 37–45.

36. Donnio, B.; Buathong, S.; Bury, I.; Guillon, D. Liquid crystalline dendrimers. Chem. Soc. Rev. 2007, 36, 1495–1513.

37. Marcos, M.; Martín-Rapún, R.; Omenat, A.; Serrano, J.L. Highly congested liquid crystal structures: Dendrimers, dendrons, dendronized and hyperbranched polymers. Chem. Soc. Rev. 2007, 36, 1889–1901.

38. Saez, I.M.; Goodby, J.W. Supermolecular liquid crystals. J. Mater. Chem. 2005, 15, 26–40.

39. Deschenaux, R.; Donnio, B.; Guillon, D. Liquid-crystalline fullerodendrimers. New J. Chem. 2007, 31, 1064–1073.

40. Gehringer, L.; Bourgogne, C.; Guillon, D.; Donnio, B. Liquid-Crystalline Octopus Dendrimers: Block Molecules with Unusual Mesophase Morphologies. J. Am. Chem. Soc. 2004, 126, 3856–3867.

41. Gehringer, L.; Guillon, D.; Donnio, B. Liquid Crystalline Octopus: An Alternative Class of Mesomorphic Dendrimers. Macromolecules 2003, 36, 5593–5601.

42. Meier, H.; Lehmann, M. Stilbenoid Dendrimers. Angew. Chem. Int. Ed. 1998, 37, 643–645.

43. Pesak, D.J.; Moore, J.S. Columnar Liquid Crystals from Shape-Persistent Dendritic Molecules. Angew. Chem. Int. Ed. Engl. 1997, 36, 1636–1639.

44. Li, J.-F.; Crandall, K.A.; Chu, P.; Percec, V.; Petschek, R.G.; Rosenblatt, C. Dendrimeric Liquid Crystals: Isotropic−Nematic Pretransitional Behavior. Macromolecules 1996, 29, 7813–7819.

45. Percec, V.; Chu, P.; Ungar, G.; Zhou, J. Rational Design of the First Nonspherical Dendrimer Which Displays Calamitic Nematic and Smectic Thermotropic Liquid Crystalline Phases. J. Am. Chem. Soc. 1995, 117, 11441–11454.

46. Goossens, K.; Lava, K.; Bielawski, C.W.; Binnemans, K. Ionic Liquid Crystals: Versatile Materials. Chem. Rev. 2016, 116, 4643–4807.

47. Donnio, B. Liquid–crystalline metallodendrimers. Inorg. Chim. Acta 2014, 409, 53–67.

48. Kato, T.; Mizoshita, N.; Kishimoto, K. Functional Liquid-Crystalline Assemblies: Self-Organized Soft Materials. Angew. Chem. Int. Ed. 2006, 45, 38–68.

49. Schnabel, W.J.; Rätz, R.; Kober, E. The Synthesis of Substituted Melams. J. Org. Chem. 1962, 27, 2514–2519.

50. Thurston, J.T.; Dudley, J.R.; Kaiser, D.W.; Hechenbleikner, I.; Schaefer, F.C.; Holm-Hansen, D. Cyanuric Chloride Derivatives. I. Aminochloro-s-triazines. J. Am. Chem. Soc. 1951, 73, 2981–2983.

51. Takagi, K.; Hattori, T.; Kunisada, H.; Yuki, Y. Triazine dendrimers by divergent and convergent methods. J. Polym. Sci. A Polym. Chem. 2000, 38, 4385–4395.

52. Lai, L.-L.; Wang, L.-Y.; Lee, C.-H.; Lin, Y.-C.; Cheng, K.-L. Nanomaterials of Triazine-Based Dendrons: Convergent Synthesis and Their Physical Studies. Org. Lett. 2006, 8, 1541–1544.

53. Steffensen, M.B.; Hollink, E.; Kuschel, F.; Bauer, M.; Simanek, E.E. Dendrimers based on [1,3,5]-triazines. J. Polym. Sci. A Polym. Chem. 2006, 44, 3411–3433.

54. Lai, L.-L.; Lee, C.-H.; Wang, L.-Y.; Cheng, K.-L.; Hsu, H.-F. Star-Shaped Mesogens of Triazine-Based Dendrons and Dendrimers as Unconventional Columnar Liquid Crystals. J. Org. Chem. 2008, 73, 485–490.

55. Kotha, S.; Kashinath, D.; Kumar, S. Synthesis of liquid crystalline materials based on 1,3,5-triphenylbenzene and 2,4,6-triphenyl-1,3,5-s-triazine. Tetrahedron Lett. 2008, 49, 5419–5423.

56. Thiebaut, O.; Bock, H.; Grelet, E. Face-on Oriented Bilayer of Two Discotic Columnar Liquid Crystals for Organic Donor−Acceptor Heterojunction. J. Am. Chem. Soc. 2010, 132, 6886–6887.

57. Shearman, G.C.; Yahioglu, G.; Kirstein, J.; Milgrom, L.R.; Seddon, J.M. Synthesis and phase behaviour of β-octaalkyl porphyrins. J. Mater. Chem. 2009, 19, 598–604.

58. Yang, C.-W.; Hsia, T.-H.; Chen, C.-C.; Lai, C.-K.; Liu, R.-S. Synthesis and Columnar Mesophase of Fluorescent Liquid Crystals Bearing a C2-Symmetric Chiral Core. Org. Lett. 2008, 10, 4069–4072.

59. Li, Z.; Zhi, L.; Lucas, N.T.; Wang, Z. Triangle-shaped polycyclic aromatics based on tribenzocoronene: Facile synthesis and physical properties. Tetrahedron 2009, 65, 3417–3424.

60. Lai, L.-L.; Hsu, S.-J.; Hsu, H.-C.; Wang, S.-W.; Cheng, K.-L.; Chen, C.-J.; Wang, T.-H.; Hsu, H.-F. Formation of Columnar Liquid Crystals on the Basis of Unconventional Triazine-Based Dendrimers by the C3-Symmetric Approach. Chem. Eur. J. 2012, 18, 6542–6547.

61. Alfa Aesar. Research Chemicals, Metals and Materials; Alfa Aesar: Ward Hill, MA, USA, 2011; p. 124.

62. Lai, L.L.; Wang, S.W.; Cheng, K.L.; Lee, J.J.; Wang, T.H.; Hsu, H.F. Induction of the columnar phase of unconventional dendrimers by breaking the C2 symmetry of molecules. Chem. Eur. J. 2012, 18, 15361–15367.

63. Lai, L.-L.; Hsieh, J.-W.; Cheng, K.-L.; Liu, S.-H.; Lee, J.-J.; Hsu, H.-F. A Small Change in Central Linker Has a Profound Effect in Inducing Columnar Phases of Triazine-Based Unconventional Dendrimers. Chem. Eur. J. 2014, 20, 5160–5166.

64. Tsai, M.-J.; Hsieh, J.-W.; Lai, L.-L.; Cheng, K.-L.; Liu, S.-H.; Lee, J.-J.; Hsu, H.-F. Converting Nonliquid Crystals into Liquid Crystals by N-Methylation in the Central Linker of Triazine-Based Dendrimers. J. Org. Chem. 2016, 81, 5007–5013.

65. Lee, C.-H.; Huang, C.-C.; Li, C.-Y.; Lai, L.-L.; Lee, J.-J.; Hsu, H.-F. Both increasing the Iso-to-Col transition and lowering the solidifying temperatures of a triazine-based dendrimer by introducing CN polar groups in the dendritic core. J. Mater. Chem. C 2019, 7, 14232–14238.

66. Castelar, S.; Barberá, J.; Marcos, M.; Romero, P.; Serrano, J.-L.; Golemme, A.; Termine, R. Supramolecular dendrimers based on the self-assembly of carbazole-derived dendrons and triazine rings: Liquid crystal, photophysical and electrochemical properties. J. Mater. Chem. C 2013, 1, 7321–7332.